Advanced Composite Materials
Publication details, including instructions for authors and subscription information:
http://www.tandfonline.com/loi/tacm20

Damage development in glass-fibre-reinforced polymers (GFRP) under transverse loading

T. Kuboki , P.-Y. B. Jar & J. J. R. Cheng

Version of record first published: 02 Apr 2012.

To cite this article: T. Kuboki , P.-Y. B. Jar & J. J. R. Cheng (2005): Damage development in glass-fibre-reinforced polymers (GFRP) under transverse loading, Advanced Composite Materials, 14:2, 131-145

To link to this article: http://dx.doi.org/10.1163/1568551053970645

Adv. Composite Mater., Vol. 14, No. 2, pp. 131–145 (2005)

Also available online - www.vsppub.com

Damage development in glass-fibre-reinforced polymers (GFRP) under transverse loading

T. KUBOKI [1,2,*], P.-Y. B. JAR [1] and J. J. R. CHENG [2]

[1] *Department of Mechanical Engineering, University of Alberta, Edmonton, AB, Canada, T6G 2G8*
[2] *Department of Civil and Environmental Engineering, University of Alberta, Edmonton, AB, Canada, T6G 2G7*

Received 12 April 2004; accepted 9 October 2004

Abstract—Objectives of the work are to use optical microscopy to identify matrix cracks that lead to delamination in cross-ply glass-fibre-reinforced polymers (GFRP) under transverse loading and to provide evidence on the associated damage evolvement procedure. Sequence of the damage evolvement was established by examining a series of identical specimens that had been subjected to different levels of loading. The results were found to be consistent with those reported in the literature, that the transverse loading generated both bending and shear cracks in the matrix, and that it was the shear cracks that initiate the delamination. What was revealed in the current study is that delamination in the bottom half of the cross section, i.e. away from the contact surface, developed first, from shear cracks in regions of mid-thickness. Only after the load was further increased was delamination in the top half of the cross-section developed, from cracks generated by stress concentration around the contact area. The study also showed that the matrix shear cracking can 'cut through' the fibre bundle in the lamina of the central region, for further growth of the shear cracks or development of delamination towards the back surface. On some occasions, growth of the shear cracks appears to be continuous under the microscopic observation, not interrupted by the cross-ply fibre lay-up.

Keywords: GFRP; transverse loading; matrix cracking; delaminations; indentation.

1. INTRODUCTION

Glass-fibre-reinforced polymers (GFRP) are now widely used for secondary structural components. The composites provide significant improvement in corrosion resistance and design flexibility, but their strength is limited by the in-plane fibre reinforcement. As a result, delamination between the fibre-reinforced layers, which often occurs unexpectedly by transverse loading during manufacturing, operation and maintenance, can cause severe structural degradation.

*To whom correspondence should be addressed. E-mail: tkuboki@ualberta.ca

The importance of the subject has attracted many recent studies. Samples of review papers are given in references [1–4]. It is now well known that the major damage mode in GFRP generated by transverse loading is delamination that occurs in the interlaminar regions. In addition to delamination, matrix cracking and indentation damage also occur, but their effect on the integrity of the GFRP structures is deemed to be limited. As a result, many studies have been devoted to the characterization of delamination resistance [5–16] and understanding of the other damage mechanisms that lead to the delamination. For the latter, previous studies have suggested that matrix cracking and delamination are strongly related [17–20]. It has even been suggested that it is the matrix cracking that leads to the delamination for carbon-fibre-reinforced epoxy (CFRP) [21–27]. Choi *et al.* [22] applied low-velocity line impact to CFRP with different ply orientations to simplify the damage mode, and examined the damage developed using photography and X-ray radiography. They suggested that delamination is always accompanied by a 'critical' matrix crack. Transverse loading can generate two types of matrix cracking, namely, bending cracks and shear cracks. The former appear to grow along the thickness direction, but the latter at an inclined angle of around 45 degrees. Hull and Shi [25] examined barely-visible impact damage (BVID) for CFRP, and proposed that shear cracks are diverted into delamination; while other studies suggested that bending cracks lead to delamination in the tension mode (mode I) [26–29] and shear cracks to delamination in pure in-plane shear mode (mode II) [26] or combined in-plane and out-of-plane shear mode (mode III) [27]. Liu *et al.* performed numerical calculation, based on their analytical model, to simulate the response of laminated composites under quasi-static transverse line loading [26] and transverse point loading [27]. They suggested that the dominant mode for delamination growth induced by bending cracks is mode I, and that by shear cracks is mode II or combination of modes II and III. It was found that the delamination resistance for CFRP is very different between mode I and mode II [30, 31].

GFRP is also known to have different delamination resistance in different modes. For example, for GFRP with isophthalic polyester as the matrix, critical strain energy release rates in mode I (G_{IC}) and in mode II (G_{IIC}) are 436 and 2754 J/m^2, respectively, measured from the non-linear point at the load–displacement curve. Since the GFRP shows very different delamination resistance between the two modes, it is essential to clarify which delamination mode dominates the damage development under transverse loading so that proper design criteria can be applied to meet the performance requirement. In this paper, optical microscopy was used to examine the type of matrix cracking that leads to delamination and the associated damage evolvement process, in cross-ply GFRP under transverse loading. The study is the first step to identify the dominant mode for delamination growth in the GFRP.

2. EXPERIMENTAL

Flat GFRP panels of 220 × 220 mm^2 were moulded in a wet hand lay-up process using isophthalic polyester (TMR300, provided by Viking Plastics, Edmonton) as the matrix and unidirectional glass fibre fabric of 0.3046 kg/m^2 (9 oz/yd^2, provided by ZCL Composites, Edmonton) as the reinforcement. The fibre lay-up was $[(0/90)_6]_s$, with nominal thickness of 6.5 mm. Overall fibre volume fraction was around 44%, estimated based on the following equation [32].

$$V_f(\%) = \frac{FAW \times N \times 100}{FD \times 2h},$$

where *FAW* is area weight of the glass fibre fabric (0.3046 kg/m^2), *N* number of fibre layers (equal to 24 in this study), *FD* fibre density (2560 kg/m^3), and 2*h* specimen thickness (0.0065 m). This fibre volume fraction is much lower than that of conventional CFRP, but is common for GFRP used for structural applications. Square specimens of 98 × 98 mm^2 were machined from the flat panels, and were used for tests under transverse loading.

It should be noted that the unidirectional glass fibre fabric consists of fibre bundles of around 1 mm in width, separated by a gap of around 1 mm using stitching threads. Details of the information were reported in reference [33]. Due to the gap between the fibre bundles, resin-rich zones also exist in the intra-laminar, inter-fibre-bundle regions.

Quasi-static indentation tests were conducted using an Instron Universal Testing Machine, at a cross-head speed of 1.27 mm/min for loading and 12.7 mm/min for unloading. The specimen was firstly clamped using a pneumatic clamp device with a central circular hole of 76.2 mm in diameter, provided by Instron, and then loaded using a cylindrical steel indenter with spherical nose of 12.7 mm in diameter. The test set-up was based on recommendations given in ASTM Standard D3763-02 [34]. Indentation force was recorded using a load-cell connected to the cylindrical indenter, and deflection of the specimen (named displacement) was measured based on the cross-head movement. The maximum force used for the indentation tests was 7.4 kN that was determined based on our previous experience to produce delamination with reasonable size in the centre of the specimen.

A water-based fluorescent penetrant (ZL-56 by ZYGLO) was used to facilitate photography of the surface cracks which, when illuminated by an ultraviolet lamp (BLACK-RAY B-100A), enhanced the contrast between the cracks and the surrounding area. Excessive fluorescent penetrant was flushed away by water, without the use of any developer to accelerate the penetrant bleed-out process. For the examination of through-thickness damages, a Zeiss optical microscope with reflected light was used. The specimens were carefully sectioned in the 90-degree direction near the indentation contact point, i.e. perpendicular to the fibre in the surface layer of Fig. 1. The cross section was then polished using 600-grit wet sandpaper and then alumina/water mixture until a mirror-like surface finish was

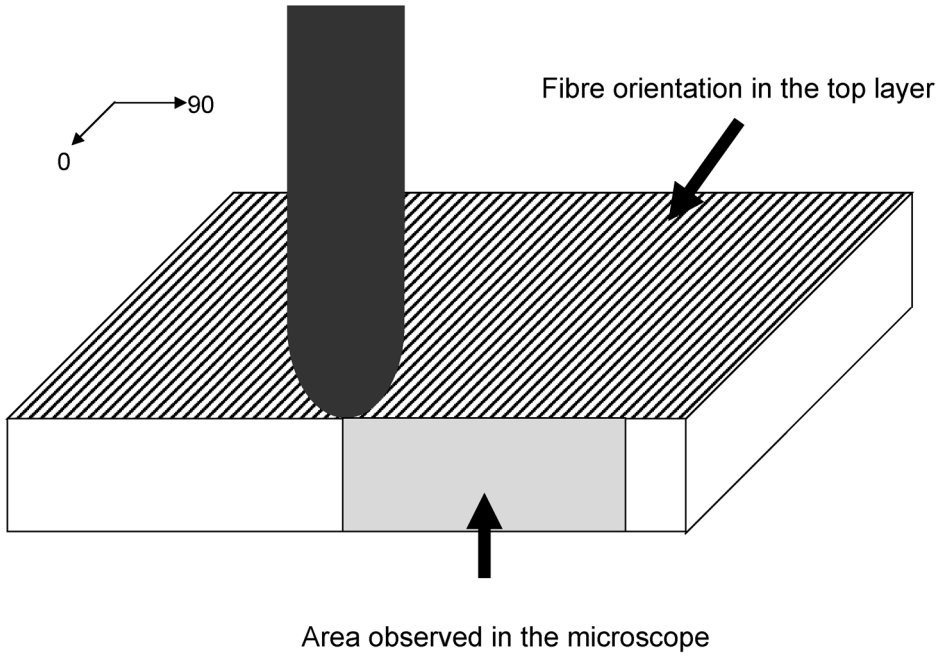

Figure 1. Relative position of indenter and the cross-section for microscopic observation. The lines on the top surface are oriented in the direction of fibre in the top layer (0-degree layer).

achieved. Since the load–displacement curves were very reproducible for this type of test, only one specimen was tested for each loading level.

3. RESULTS

Figure 2 shows the typical load–displacement curve of the GFRP specimens used in this study. Each of points A to F marked on the curve, corresponding to loads at 2.3, 3.4, 4.7, 5.0, 5.5 and 7.3 kN, respectively, was the maximum load used for the damage development. All specimens used in the study were unloaded immediately after the desired loads were reached. A transitional point exists on the loading curve (around point C in Fig. 2) where a significant drop of the curve slope occurs. As suggested by Davallo *et al.* [35], the slope drop was caused by the on-set of delamination. Therefore, no delamination was expected for specimens loaded to points A and B in Fig. 2, which will be discussed in Fig. 4, but delamination should be visible from back surface (bottom surface in Fig. 1) of specimens loaded to the rest of the points in Fig. 2, which will be discussed in Figs. 5 to 8. The specimen for point C, which is just beyond the on-set of delamination, was expected to contain damage in a very early stage of the delamination development, which will be discussed in Fig. 5.

Photographs of the front surface (top surface in Fig. 1) and the back surface from specimens tested to each of the points in Fig. 2 are summarised in Fig. 3. The

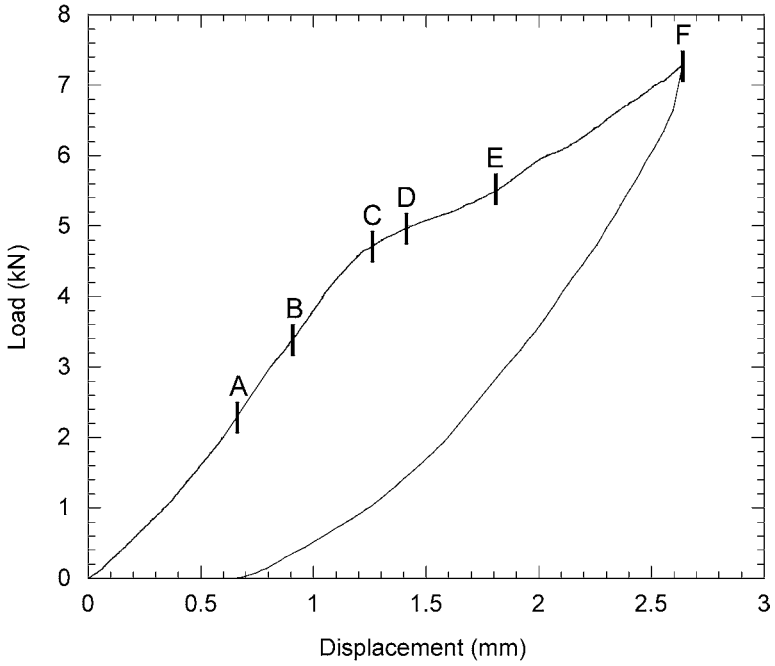

Figure 2. Typical load-displacement curve under the static loading, on which points A to F indicate the maximum loading level used for Figs 4–8.

photographs have been arranged in such a way that fibre in the surface layer is in the vertical direction. Photographs on the top row of Fig. 3 were from the front surfaces with the centre being the indentation point, and the middle row from the back surfaces. Photographs in the bottom row were also from the back surfaces, but with the fluorescent penetrant treatment so that bending cracks that run in the vertical direction around the centre of the photographs could be seen clearly.

Damage appeared on surfaces of specimens loaded to points A and B, although at these loading levels, no slope change has been detected on the loading curve. Damage on the front surfaces (the two left photographs in the top row of Fig. 3) was caused by indentation, and that on the back surfaces (the two left photographs in the bottom row of Fig. 3) are short bending cracks, as identified by cross-section examination in Fig. 4, which extend in the vertical direction. These bending cracks are hardly visible without the assistance of fluorescent penetrant, as shown by the two left photographs in the middle row of Fig. 3. It should be noted that the fluorescent penetrant also enhanced the contrast between the stitch threads and the matrix, showing the stitch threads as a pattern of square mesh on the photographs.

As expected, delamination did not show on the back surfaces of specimens that had been loaded to points A and B, but did on specimens loaded to points C, D, E, and F, for which evidence, presented in Figs 4 to 8, will be discussed later. Since damage appearing on the specimen loaded to point D was very similar to that shown

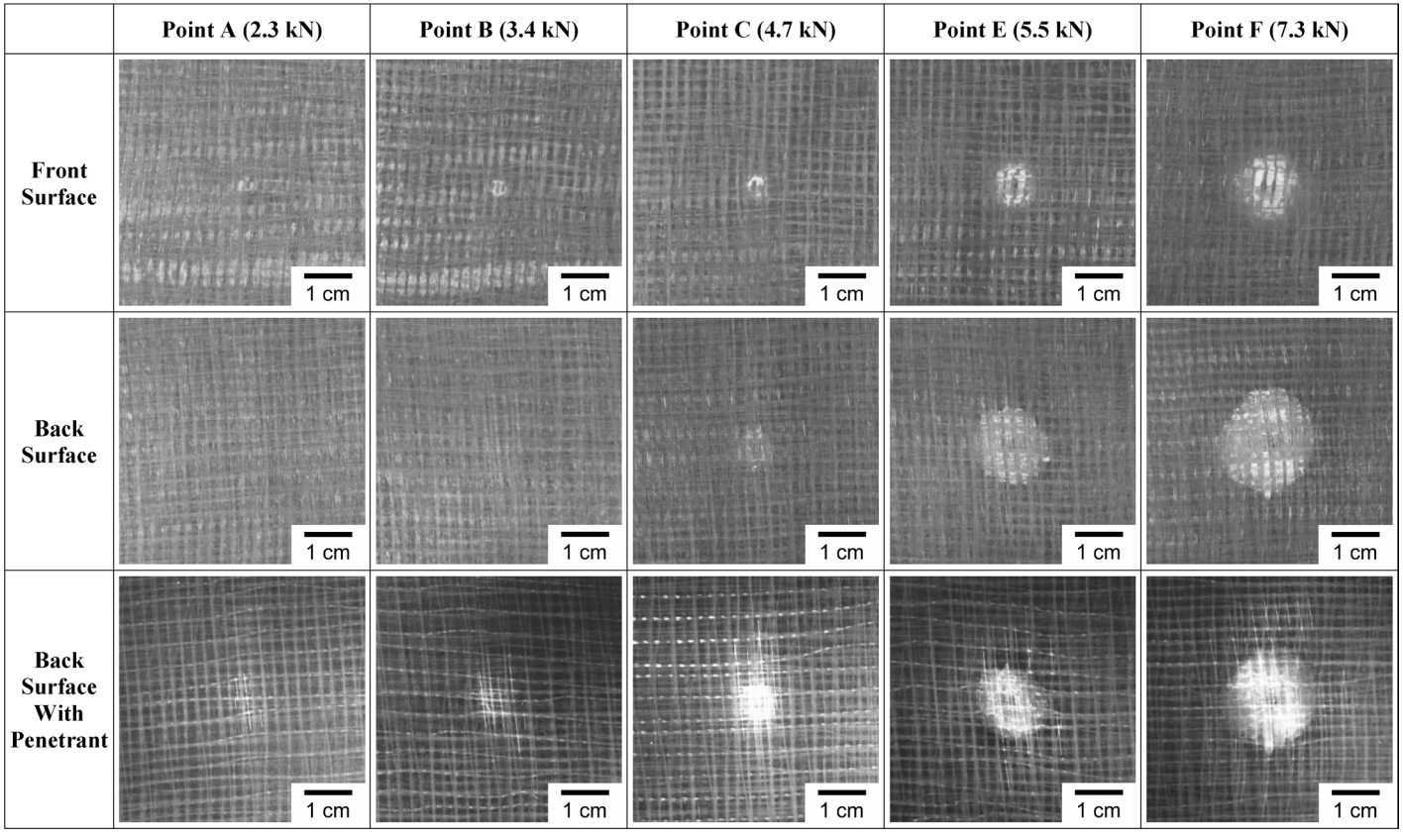

Figure 3. Optical photographs of specimens tested under transverse loading, with the maximum loading levels indicated in Fig. 2.

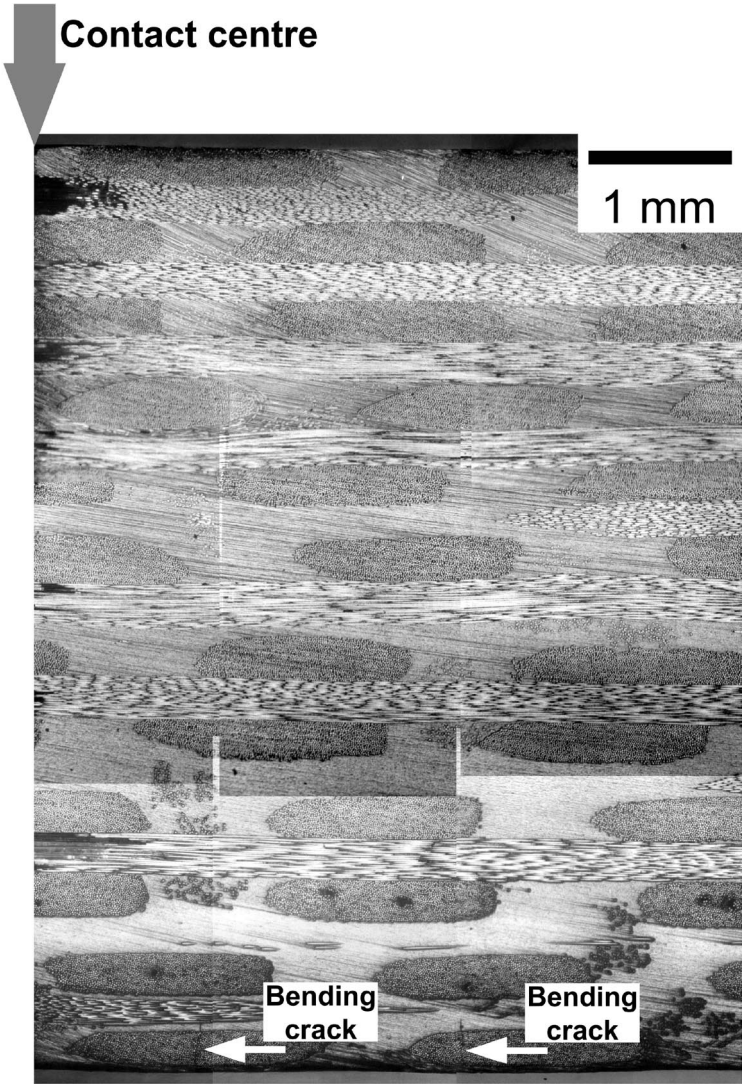

Figure 4. Composite optical micrograph for cross-section of a specimen loaded to point B in Fig. 2.

by the specimen loaded to point C, its photographs were omitted from Fig. 3. As shown by these photographs, the increase of load increased the size of delamination.

Figure 4 is a composite optical micrograph that shows the damage pattern through the cross-section of a specimen after being loaded to point B in Fig. 2. As indicated in Fig. 1, the cross-section is taken in parallel to the 90-degree direction, i.e. perpendicular to the fibre in the surface layers. The top line of the micrograph in Fig. 4 corresponds to the front surface, with an arrow indicating the contact centre. Fibre bundles in the 0-degree direction appear to have an elliptical shape with the major axis in the horizontal direction. The micrograph contains two bending cracks

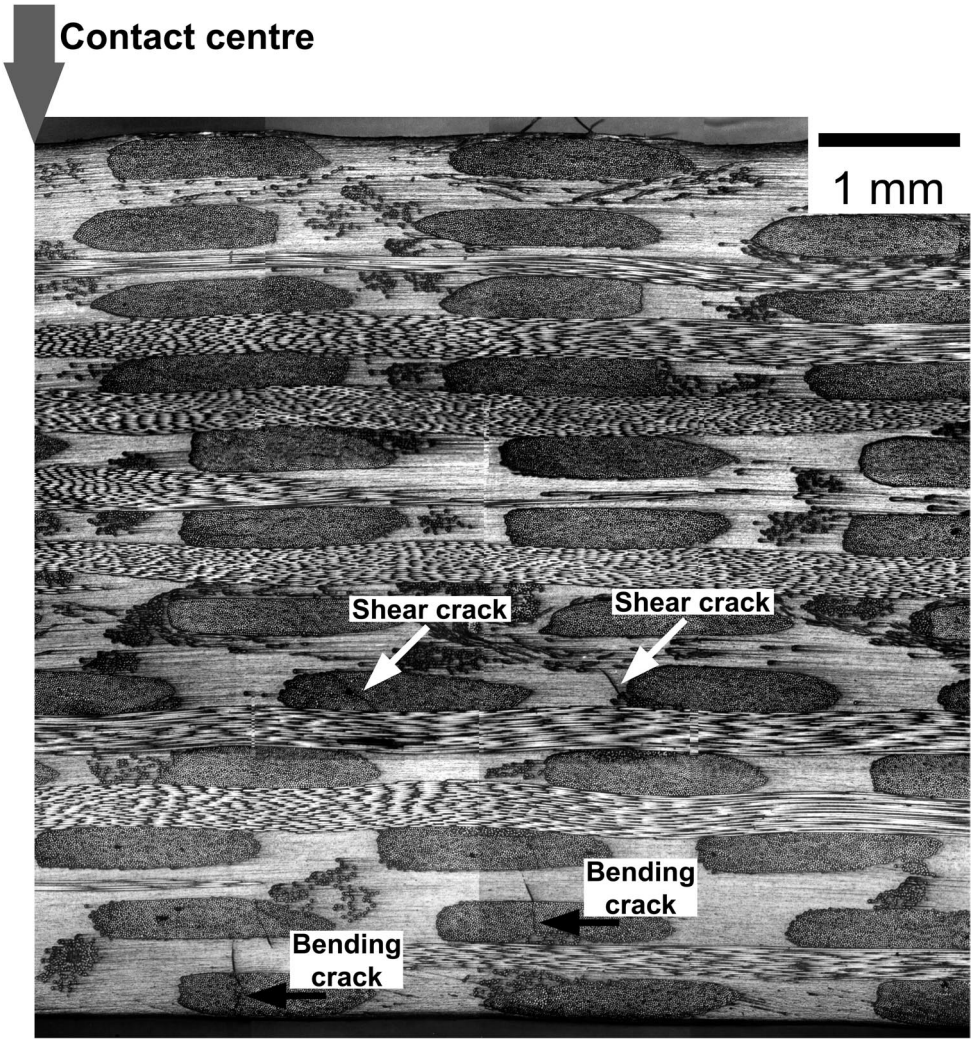

Figure 5. Composite optical micrograph for cross-section of a specimen loaded to point C in Fig. 2.

at the bottom, as indicated by two arrows, occurring within the fibre bundles of the first layer from the back surface. However, the micrograph could not be used to identify the origin of the surface indentation, as the damage generated by the surface indentation is believed to consist of very small cracks. Further study will be required to identify the surface indentation and its associated damage. It should be noted that the dark elliptical region underneath the contact point are artefacts, caused by dust being deposited on the surface.

The micrograph of the cross-section from the specimen loaded to point C is shown in Fig. 5. Although the loading corresponded to that for the onset of delamination, the micrograph in Fig. 5 only showed some shear cracks without any indication of delamination. In addition, bending cracks in Fig. 5 have extended to the 3rd

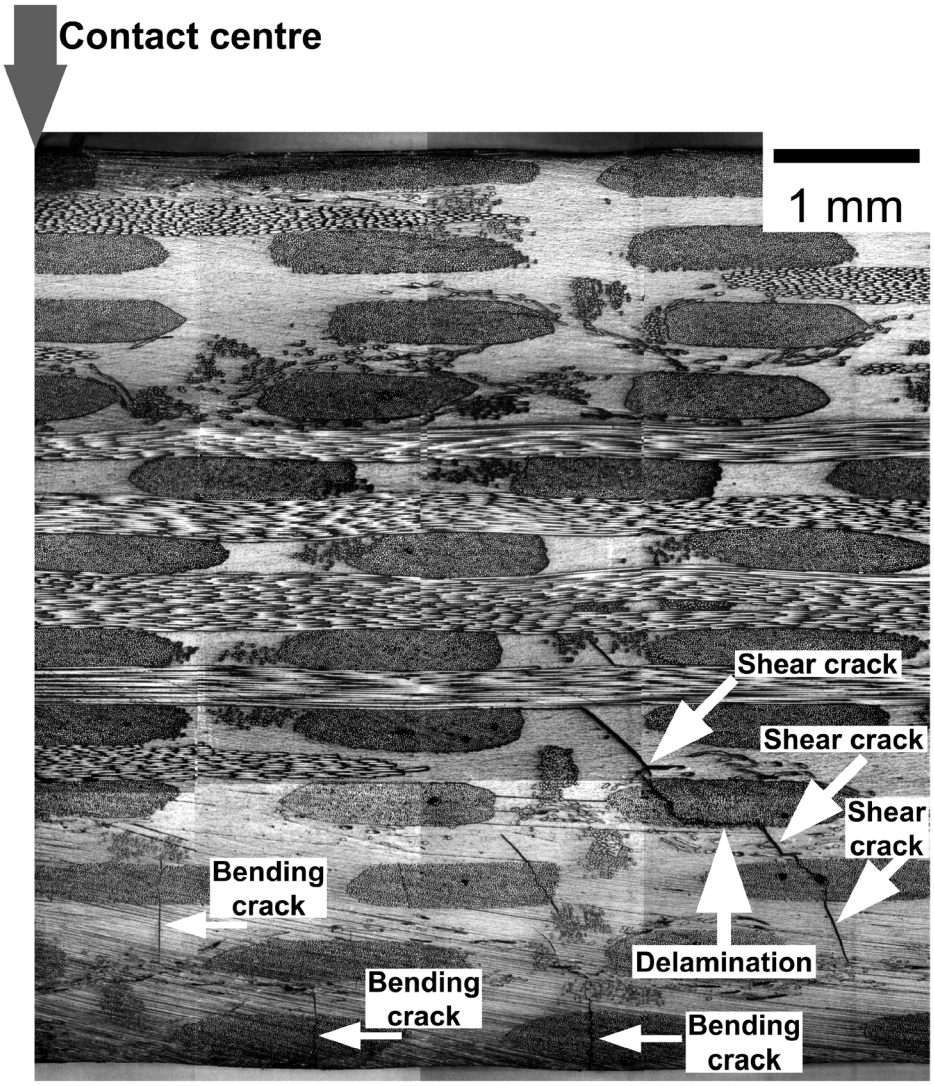

Figure 6. Composite optical micrograph for cross-section of a specimen loaded to point D in Fig. 2.

layer from the back surface. It should be noted that the search for delamination cracks in this specimen was not limited to one cross-section. Several cross-sections were prepared, but none of them showed any trace of delamination. Therefore, it is believed that the so-called delamination pattern shown on the back surface of the specimen, as depicted by the middle photograph in the bottom row of Fig. 3, is a collective image on the specimen surface, projected from many shear cracks without the presence of any delamination crack.

However, delamination cracks were indeed observed in the specimen loaded to point D, as shown in Fig. 6 that also shows an increase in the extent of growth of

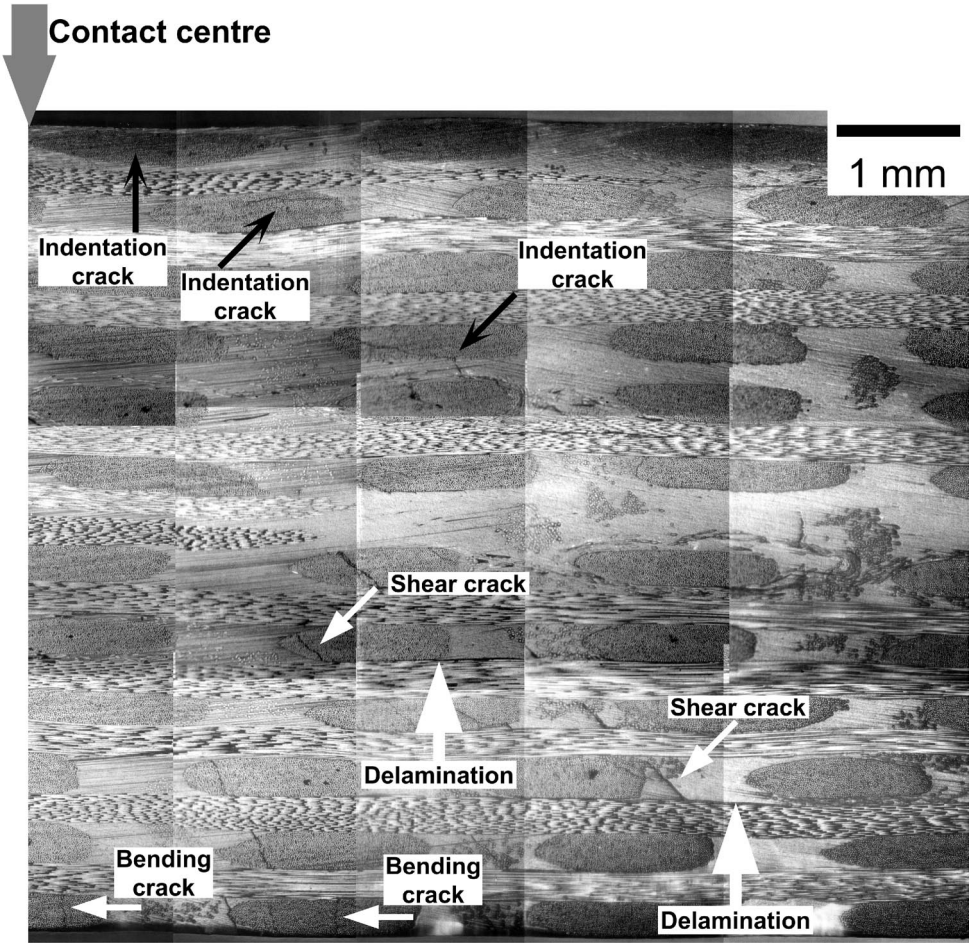

Figure 7. Composite optical micrograph for cross-section of a specimen loaded to point E in Fig. 2.

shear cracks. Figure 6 shows that the delamination cracks were only connected to shear cracks, and occurred only in the bottom half of the cross section. Further increase of the load to point E enhanced the development of shear and delamination cracks in the bottom half of the cross section, as shown in Fig. 7. On the contrary, development of the bending cracks was limited. Figure 7 also shows that cracks in the top half of the cross section started appearing, which were possibly originated from stress concentration around the contact indentation. Since the stress profile around the contact indentation is complicated, the cracks generated in this region do not grow in a particular direction, unlike the growth of bending and shear cracks. In the rest of the text, cracks originated from stress concentration around the contact indentation are referred to as 'indentation cracks'.

Further increase of the load to point F in Fig. 2 increased the area of the cross-section that contained shear and delamination cracks, as shown in Fig. 8. The

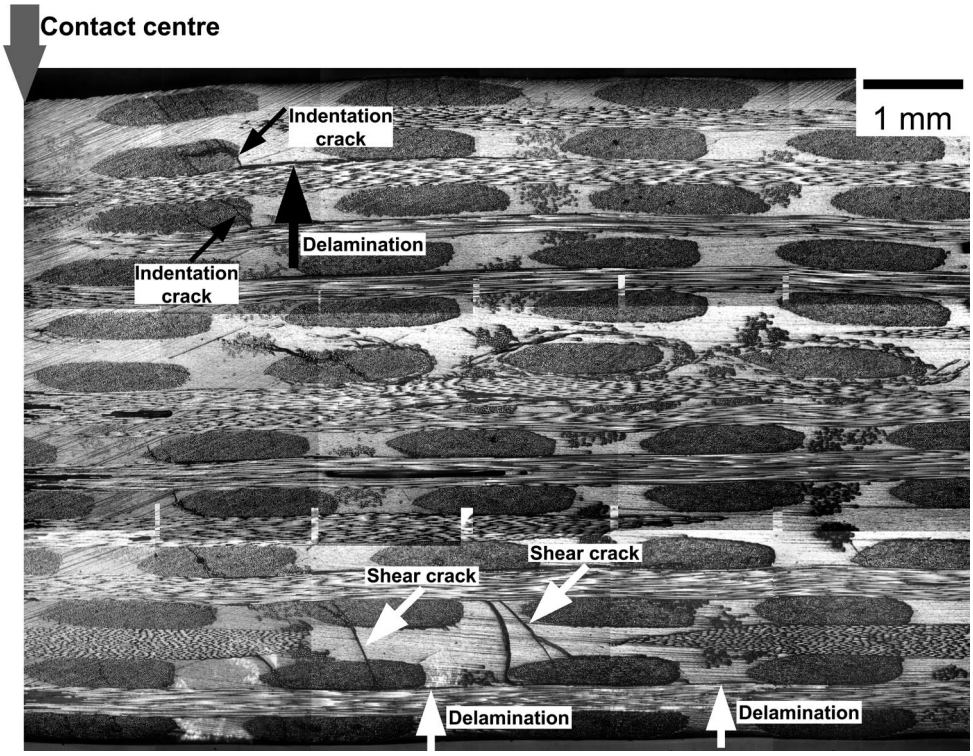

Figure 8. Composite optical micrograph for cross-section of a specimen loaded to point F in Fig. 2.

development of delamination on the top half of the cross-section is believed to be related to the increase of damage size seen from the front surface, as shown by the right photograph in the top row of Fig. 3.

It should be noted that though these composite micrographs were taken from different specimens, repeatability of the fracture behaviour was carefully checked, and the fracture development process was found to be highly consistent.

4. DAMAGE DEVELOPMENT PROCESS

The microscopic observations suggest that the first damage modes under the transverse loading were bending cracks and surface indentation that occurred in a very early stage of loading, though their occurrence could not be detected on the load–displacement curve. Shear cracks occurred much later, starting from the central layers towards the back surface. The study showed that it was the shear cracks that led to delamination that caused a significant change in the slope of the load–displacement curve. Further increase of the load initiated delamination from the indentation cracks in the top half of the cross-section. Cantwell and Morton [36] also observed the indentation-induced delamination in thick CFRP, but it was not clear which matrix-cracking mode, i.e. bending or shear, was

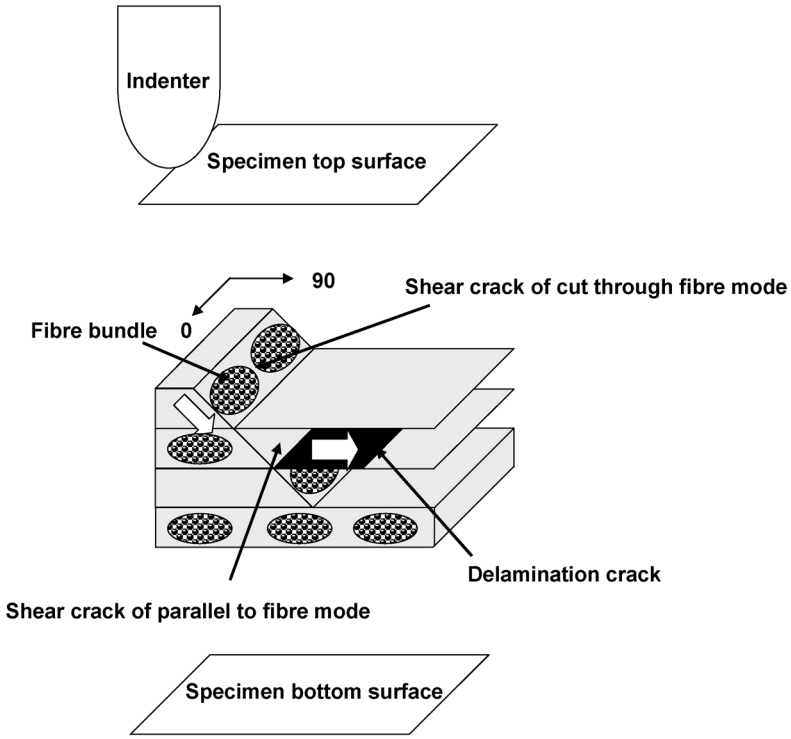

Figure 9. Schematic drawing of the development of shear cracks and delamination in the bottom half of the cross-section.

responsible for the delamination in the bottom half of the cross-section, as that shown in Fig. 6. The current study suggests that the shear cracking is the main mechanism for the delamination. The results also suggest that the shear-crack-induced delamination only occurred in the bottom half of the cross-section, and could take place independently from the indentation-induced delamination that occurred in the top half of the cross-section.

The mechanisms for the formation of shear cracks, followed by delamination, are depicted in Fig. 9. Due to resin-rich regions between the fibre bundles, surface of the shear cracks can either be in parallel to the fibre or 'cut through' the fibre bundles, as demonstrated in Fig. 9 in which the shear crack formed in the upper layer belongs to the latter (cut-through fibre) mode and the shear crack formed in the lower layer belongs to the former (parallel to fibre) mode. White arrows in the figure indicate the possible directions of crack growth. The proposed process for crack development is consistent with that proposed by Hull and Shi [25], though their model did not point out that shear cracks in the mid-layer were only responsible for the delamination in the bottom half of the cross-section. Delamination on the top half of the cross-section was an extension of indentation cracks.

It should be noted that as a result of the proposed damage development process, a shear crack can appear to grow continuously downward through layers of 0° and

90° fibre, but a delamination crack can only be generated in the interlaminar region that has upper layer with fibre perpendicular to the crack growth direction and lower layer with fibre parallel to the crack growth direction.

Another interesting phenomenon observed in the study is that the bending cracks and shear cracks were formed independently from each other. That is, the bending cracks were generated from the bottom surface in a very early stage of loading but the development was limited. On the other hand, shear cracks were initiated from the middle layers in a much later stage, and resulted in a significant drop of the slope of the load–displacement curve. The delamination cracks were found to connect to the shear cracks, not the bending cracks, as shown in Figs 6, 7 and 8. This suggests that bending cracks were not associated with the delamination formation.

Several studies in the past have suggested that when subjected to transverse loading, load–displacement curve of fibre composites is virtually insensitive to loading rate in the range of static to low-speed impact [37–41]. Therefore, it is believed that mechanisms of the delamination formation proposed in the current study are also applicable to the GFRP when subject to low-speed impact.

5. CONCLUSIONS

Matrix cracks that lead to delamination in cross-ply GFRP when subjected to transverse loading and the associated delamination evolvement process were studied using optical microscopy. The results showed that under loading, bending cracks and contact indentation were developed first. Shear cracks, on the other hand, required a much higher loading level, but led to delamination that caused a significant drop of slope of the load–displacement curve. This process of delamination development was found to occur at the bottom half of the cross-section. Indentation cracks also induced delamination that occurred on the top half of the cross-section.

Acknowledgements

The work was sponsored by the ISIS Canada and the Natural Sciences and Engineering Research Council of Canada (NSERC). We are grateful to B. Faulkner, A. Yuen and T. Hilvo in the Department of Mechanical Engineering, University of Alberta for their technical assistance.

REFERENCES

1. W. J. Cantwell and J. Morton, The impact resistance of composite materials — a review, *Composites* **22**, 347–362 (1991).
2. S. Abrate, Impact on laminated composite materials, *Appl. Mech. Rev.* **44**, 155–190 (1991).
3. S. Abrate, Impact on laminated composites: Recent advances, *Appl. Mech. Rev.* **47**, 517–544 (1994).
4. M. O. W. Richardson and M. J. Wisheart, Review of low-velocity impact properties of composite materials, *Composites: Part A* **27A**, 1123–1131 (1996).

5. J. E. Masters, Correlation of impact and delamination resistance in interleafed laminates, in: *Proceedings of 6th International Conference on Composite Materials and Second European Conference on Composite Materials (ICCM-6 & ECCM-2)*, F. L. Matthews, N. C. R. Buskell, J. M. Hodgkinson and J. Morton (Eds), Vol. 3, pp. 3.96–3.107 (1987).
6. J. E. Masters, Characterization of impact damage development in graphite/epoxy laminates, in: *Fractography of Modern Engineering Materials: Composites and Metals, ASTM STP 948*, J. E. Masters and J. J. Au (Eds), pp. 238–258. American Society for Testing and Materials, Philadelphia (1987).
7. H. Y. T. Wu and G. S. Springer, Measurements of matrix cracking and delamination caused by impact on composite plates, *J. Compos. Mater.* **22**, 518–532 (1988).
8. H. Y. T. Wu and G. S. Springer, Impact-induced stresses, strains, and delaminations in composite plates, *J. Compos. Mater.* **22**, 533–560 (1988).
9. H. Wang and T. Vu-Khanh, Impact-induced delamination in $[0_5, 90_5, 0_5]$ carbon fiber/polyetheretherketone composite laminates, *Polym. Eng. Sci.* **31**, 1301–1309 (1991).
10. C. J. Jih and C. T. Sun, Prediction of delamination in composite laminates subjected to low velocity impact, *J. Compos. Mater.* **27**, 684–701 (1993).
11. H. Razi and A. S. Kobayashi, Delamination in cross-ply laminated composite subjected to low-velocity impact, *AIAA Journal* **31**, 1498–1502 (1993).
12. S. R. Finn and G. S. Springer, Delaminations in composite plates under transverse static or impact loads — Model, *Comps. Struct.* **23**, 177–190 (1993).
13. C. T. Sun and C. J. Jih, Quasi-static modeling of delamination crack propagation in laminates subjected to low-velocity impact, *Comp. Sci. Tech.* **54**, 185–191 (1995).
14. H. Wang and T. Vu-Khanh, Fracture mechanics and mechanisms of impact-induced delamination in laminated composites, *J. Compos. Mater.* **29**, 156–178 (1995).
15. G. A. Schoeppner and S. Abrate, Delamination threshold loads for low velocity impact on composite laminates, *Composites: Part A* **31**, 903–915 (2000).
16. R. K. Luo, E. R. Green and C. J. Morrison, An approach to evaluate the impact damage initiation and propagation in composite plates, *Composites: Part B* **32**, 513–520 (2001).
17. N. Takeda, R. L. Sierakowski and L. E. Malvern, Microscopic observations of cross-sections of impacted composite laminates, *Composites Technology Review* **4**, 40–44 (1982).
18. S. P. Joshi and C. T. Sun, Impact-induced fracture in a laminated composite, *J. Compos. Mater.* **19**, 51–66 (1985).
19. D. Liu and L. E. Malvern, Matrix cracking in impacted glass/epoxy plates, *J. Compos. Mater.* **21**, 594–609 (1987).
20. S. W. Lee and C. T. Sun, A quasi-static penetration model for composite laminates, *J. Compos. Mater.* **27**, 251–271 (1993).
21. C. T. Sun and S. Rechak, Effect of adhesive layers on impact damage in composite laminates, in: *Composite Materials: Testing and Design (Eighth Conference), ASTM STP 972*, J. D. Whitcomb, (Ed.), pp. 97–123. American Society for Testing and Materials, Philadelphia (1988).
22. H. Y. Choi, R. J. Downs and F. K. Chang, A new approach toward understanding damage mechanisms and mechanics of laminated composites due to low-velocity impact: Part I — Experiments, *J. Compos. Mater.* **25**, 992–1011 (1991).
23. H. Y. Choi, H. Y. T. Wu and F. K. Chang, A new approach toward understanding damage mechanisms and mechanics of laminated composites due to low-velocity impact: Part II — Analysis, *J. Compos. Mater.* **25**, 1012–1038 (1991).
24. H. Y. Choi and F. K. Chang, A model for predicting damage in graphite/epoxy laminated composites resulting from low velocity point impact, *J. Compos. Mater.* **26**, 2134–2169 (1992).
25. D. Hull and Y. B. Shi, Damage mechanism characterization in composite damage tolerance investigations, *Comps. Struct.* **23**, 99–120 (1993).
26. S. Liu, Z. Kutlu and F. K. Chang, Matrix cracking and delamination in laminated composite beams subjected to a transverse concentrated line load, *J. Compos. Mater.* **27**, 436–470 (1993).

27. S. Liu and F. K. Chang, Matrix cracking effect on delamination growth in composite laminates induced by a spherical indenter, *J. Compos. Mater.* **28**, 940–977 (1994).
28. G. B. Murri and E. G. Guynn, Analysis of delamination growth from matrix cracks in laminates subjected to bending loads, in: *Composite Materials: Testing and Design (Eighth Conference) ASTM STP 972*, J. D. Whitcomb (Ed.), pp. 322–339. American Society for Testing and Materials, Philadelphia (1988).
29. C. T. Sun and M. G. Manoharan, Growth of delamination cracks due to bending in a $[90_5/0_5/90_5]$ laminate, *Compos. Sci. Tech.* **34**, 365–377 (1989).
30. M. Hojo, K. Kageyama and K. Tanaka, Prestandardization study on mode I interlaminar fracture toughness test for CFRP in Japan, *Composites* **26**, 243–255 (1995).
31. K. Takaka, K. Kageyama and M. Hojo, Prestandardization study on mode II interlaminar fracture toughness test for CFRP in Japan, *Composites* **26**, 257–267 (1995).
32. European Structural Integrity Society (ESIS), Delft, The Netherlands. Protocols for interlaminar fracture testing of composites (1993).
33. T. Kuboki, T. Hilvo and P. Y. B. Jar, Detection of interlaminar cracks in fibre-reinforced polymers (FRP), *J. Mater. Sci. Lett.* **21**, 1789–1791 (2002).
34. Standard test method for high speed puncture properties of plastics using load and displacement sensors, ASTM standard D3763–02 (2002).
35. M. Davallo, M. L. Clemens, H. Taylor and A. N. Wilkinson, Low energy impact behaviour of polyester-glass composites formed by resin transfer moulding, *Plast. Rubber Compos. Proc. Appl.* **27**, 384–391 (1998).
36. W. J. Cantwell and J. Morton, Geometrical effects in the low velocity impact response of CFRP, *Comps. Struct.* **12**, 39–59 (1989).
37. W. Elber, The effect of matrix and fiber properties on impact resistance, in: *Tough Composite Materials: Recent Developments*, pp. 89–110. Noyes Publications, Park Ridge (1985).
38. P. O. Sjøblom, J. T. Hartness and T. M. Cordell, On low-velocity impact testing of composite materials, *J. Compos. Mater.* **22**, 30–52 (1988).
39. B. Z. Jang, L. C. Chen, L. R. Hwang, J. E. Hawles and R. H. Zee, The response of fibrous composites to impact loading, *Polym. Compos.* **11**, 144–157 (1990).
40. S. M. Lee and P. Zahuta, Instrumented impact and static indentation of composites, *J. Compos. Mater.* **25**, 204–222 (1991).
41. E. Wu and K. Shyu, Response of composite laminates to contact loads and relationship to low-velocity impact, *J. Compos. Mater.* **27**, 1443–1464 (1993).